Pressure-dependent Raman scattering and photoluminescence of Zn 1 x Cd x Se epilayers

Y. C. Lin, C. H. Chiu, W. C. Fan, S. L. Yang, D. S. Chuu, and W. C. Chou

Citation: Journal of Applied Physics **101**, 073507 (2007); doi: 10.1063/1.2719287
View online: http://dx.doi.org/10.1063/1.2719287
View Table of Contents: http://scitation.aip.org/content/aip/journal/jap/101/7?ver=pdfcov
Published by the AIP Publishing

Pressure-dependent Raman scattering and photoluminescence of $Zn_{1-x}Cd_xSe$ epilayers

Y. C. Lin, C. H. Chiu, W. C. Fan, S. L. Yang, D. S. Chuu, and W. C. Chou[a)]
Department of Electrophysics, National Chiao Tung University, Hsinchu 30010, Taiwan, Republic of China

(Received 15 November 2006; accepted 24 February 2007; published online 4 April 2007)

Raman and photoluminescence spectra of cubic $Zn_{1-x}Cd_xSe$ ($0 \leqq x \leqq 0.32$) epilayers were obtained at high pressure. The impurity mode *I* observed in the phonon Raman spectra at low temperature confirms the intermediate phonon mode behavior. A split transverse optical phonon mode was found in the down-stroke high-pressure Raman scattering. Additionally, the pressure-dependent longitudinal optical (LO) phonon frequencies and the Grüneisen parameter (γ_{LO}) were obtained by quadratic polynomial fitting. Pressure-driven resonant Raman scattering effect was observed in samples with a high Cd concentration ($x \geqq 0.18$). The critical pressure of semiconductor-to-metal phase transition (Pt) decreases as the Cd content increases. As the Cd concentration increases from 0 to 0.32, Pt falls from 13.6 to 9.4 GPa, according to Pt (GPa)$=13.6-6.8x-20.3x^2$. © *2007 American Institute of Physics*. [DOI: 10.1063/1.2719287]

I. INTRODUCTION

Wide-band-gap II-VI ternary compound semiconductor, $Zn_{1-x}Cd_xSe$, has attracted much attention because its tunable band gap covers the visible spectrum. The physical properties of $Zn_{1-x}Cd_xSe$ have been extensively studied over the last decade because the material is extensively employed as an active layer in ZnSe-based laser diodes.[1–4] The crystal structure of bulk $Zn_{1-x}Cd_xSe$ is zinc blende (ZB) for $x < 0.3$, wurtzite for $x > 0.7$, and is a mixture of both for $0.3 \leqq x \leqq 0.7$.[5,6] A single-phase ZB crystalline structure over the entire Cd composition range from ZnSe to CdSe (Refs. 6–8) can be grown on (001) GaAs substrates by molecular beam epitaxy (MBE). Furthermore, the energy-dispersive x-ray diffraction (EDXD) and Raman scattering of ZnSe-based II-VI ternary compounds[9–12] were investigated at high pressure to study the structural transformations. However, the pressure-induced structural transition and the crystal stability of ZB $Zn_{1-x}Cd_xSe$ epilayers under hydrostatic pressure still remain unexplored. The structural transitions from semiconductor to metal and the ZB (B_3 phase) to rocksalt (RS), (B_1 phase), were found to be consistent with the disappearance of the LO phonon from the Raman spectra.[10–13]

This work discusses the phonon Raman and photoluminescence (PL) spectra of ZB $Zn_{1-x}Cd_xSe$ epilayers ($x=0$, 0.06, 0.11, 0.18, 0.25, and 0.32) at room temperature and high pressures. The optical phonon mode behavior, pressure-dependent LO phonon frequencies, LO phonon line broadening, the splitting of the TO mode in the down-stroke pressurized process, and the Grüneisen parameter (γ_{LO}) of $Zn_{1-x}Cd_xSe$ epilayers were determined. Moreover, samples with a high ($x \geqq 0.18$) Cd content exhibit pressure-driven resonant Raman scattering (RRS) enhancement. Additionally, the critical pressure of semiconductor-to-metal phase (Pt) transition was plotted as a function of Cd content (x).

[a)]Author to whom correspondence should be addressed; electronic mail: wuchingchou@mail.nctu.edu.tw

II. EXPERIMENT

The $Zn_{1-x}Cd_xSe$ epilayers ($x=0$, 0.06, 0.11, 0.18, 0.25, and 0.32) were grown on semi-insulating GaAs (001) substrates with a Veeco Applied EPI 620 MBE system using Zn (6*N* purity), Se (6*N* purity), and Cd (6*N* purity) solid sources. The substrate temperature was maintained at 300 °C, and the thickness of the $Zn_{1-x}Cd_xSe$ epilayers was fixed at around 0.5 μm. The Cd content was determined by EDX analysis.

High-pressure measurements were taken in a gasket diamond anvil cell (DAC). The culets of the diamond anvils are 500 μm in diameter. The sample chamber was a circular hole with a diameter of about 170 μm, which was predrilled on the stainless steel gasket using an electrical discharge machine. A methanol-ethanol 4:1 mixed liquid was used as a pressure-transmitting medium in order to maintain the hydrostatic conditions. The hydrostatic pressure was determined by the spectral shift of the ruby R1 line, which is widely used in high-pressure Raman and PL measurements.[14,15] The pressure gradient was less than 0.5 GPa, as determined by measurements made at various positions of the sample chamber. Before the $Zn_{1-x}Cd_xSe$ sample was loaded into the DAC, the GaAs substrate was removed by mechanical polishing and chemical etching with $H_2O:H_2O_2:NaOH=30$ ml:21 ml:4 g.

Raman and PL spectra were performed at room temperature and collected in backscattering configuration using a 514.5 nm line of an Ar^+-ion laser as the excitation source. The spectra were analyzed by a SPEX 1404 double grating spectrometer equipped with a multichannel LN_2-cooled charge-coupled device (CCD). The 514.5 nm holographic notch filter was used to filter out the Rayleigh scattering.

III. RESULTS AND DISCUSSION

Figure 1 presents the first-order Raman spectra of $Zn_{1-x}Cd_xSe$ ($x=0$, 0.06, 0.11, 0.18, 0.25, and 0.32) epilayers. The spectra were all obtained at room temperature and am-

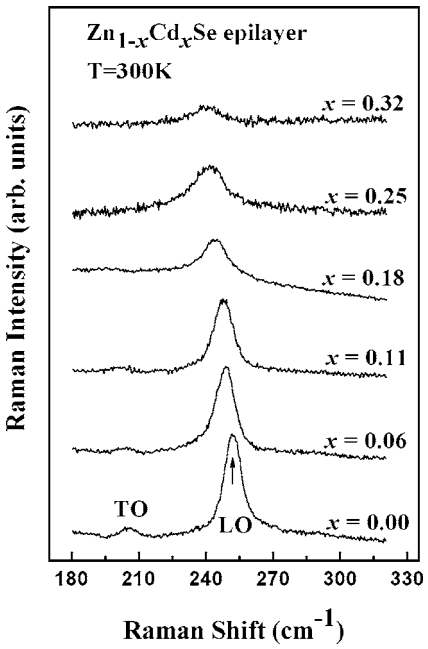

FIG. 1. Raman spectra of $Zn_{1-x}Cd_xSe$ epilayers ($0 \leqq x \leqq 0.32$) at 300 K and ambient pressure.

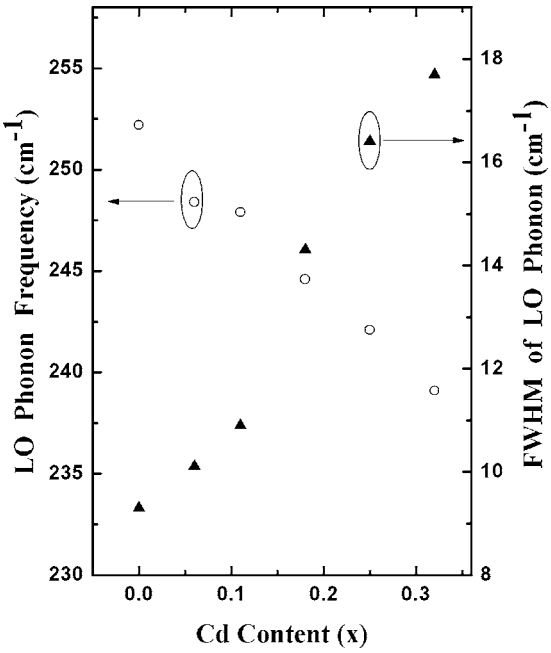

FIG. 2. Dependence of LO phonon frequencies (open circle) and FWHM (solid triangle) on Cd concentration (x).

bient pressure under $z(x+y,x+y)\bar{z}$ backscattering geometry. The Raman selection rule for this geometry forbids the TO and allows the emission of LO only. However, a weak TO feature which appears at 205.4, 203.3, and 201.6 cm^{-1} for $x=0$, 0.06, and 0.11 samples, respectively, can be attributed to a slight deviation from perfect backscattering geometry. Table I presents the LO and TO phonon frequencies and the linewidth of the LO phonons of all $Zn_{1-x}Cd_xSe$ samples. As the Cd content increases, both the LO and the TO phonon frequencies decrease. Asymmetric broadening of the peaks of the LO phonon at high Cd content ($x \geqq 0.18$) is observed, attributed primarily to the disorder of the alloy,[16] and becomes more evident under pressure. Figure 2 shows the dependence of LO phonon frequencies and the full width at half maximum (FWHM) on the Cd concentration (x) using open circles and solid triangles, respectively. The LO phonon frequency falls as x increases, and is accompanied by an increase in FWHM.

The zone-center optical phonon mode of ZB $Zn_{1-x}Cd_xSe$ was controversial in previous studies. Alonso *et al.*,[17] Avendaño-López *et al.*,[5] and Camacho *et al.*[18] found that in addition to the LO and TO phonon modes, an impurity mode

TABLE I. LO and TO phonon frequencies and FWHM of LO phonon for $Zn_{1-x}Cd_xSe$ epilayers.

Cd content (x)	LO phonon frequency (cm^{-1})	TO phonon frequency (cm^{-1})	FWHM of LO phonon (cm^{-1})
0	252.2	205.4	9.3
0.06	248.4	203.3	10.1
0.11	247.9	201.6	10.9
0.18	244.6	···	14.3
0.25	242.1	···	16.4
0.32	239.1	···	17.7

I was present, and could be attributed to the impurity modes of Zn in CdSe for x close to 1 and to that of Cd in ZnSe for x close to 0. Therefore, they concluded that $Zn_xCd_{1-x}Se$ exhibited mixed-mode behavior. However, Meredith *et al.*[16] and Li *et al.*[19] indicated that $Zn_xCd_{1-x}Se$ exhibited single mode behavior because they observed no impurity mode and their experimental results were consistent with the mass criterion of one mode behavior.[16] Although at room temperature, only LO and TO phonons of $Zn_{1-x}Cd_xSe$ ($x=0$ to $x=0.32$) are observed in the Raman spectra, as shown in Fig. 1. The low-temperature Raman scattering measurements exhibit the impurity mode *I* (Fig. 3). In particular, at $x \geqq 0.25$, under the RRS condition, the impurity mode *I* is clearly present. Moreover, the frequency of the *I* phonon falls as the Cd content increases, supporting the results given in Ref. 17. Accordingly, the vibration mode of $Zn_{1-x}Cd_xSe$ is an intermediate.

Figure 4 presents the up-stroke pressure-dependent Raman spectra of $Zn_{1-x}Cd_xSe$ epilayer ($x=0.06$) at room temperature. A strong LO phonon and a weak TO feature are observed at ambient pressure, while the TO phonon becomes more intense as the pressure increases. The $x=0$ and 0.11 samples exhibit the same behavior because the sample chips deviate from the perfect backscattering geometry when the samples are pressured in the diamond cell. The applied pressure reduces the lattice constant and the crystal volume. Therefore, the frequencies of the LO and TO phonons shift to higher frequencies, accompanied by decreases in intensity. The LO phonon disappears and the sample becomes opaque at approximately 13.0 GPa. These facts are evidence of the structural transition from the semiconductor to the metal phase. However, a TO phonon is still observed in the Raman spectra when the semiconductor becomes metallic. It can be ascribed to the fact that transverse surface lattice vibrations are allowed in both semiconductor and metal, even if the

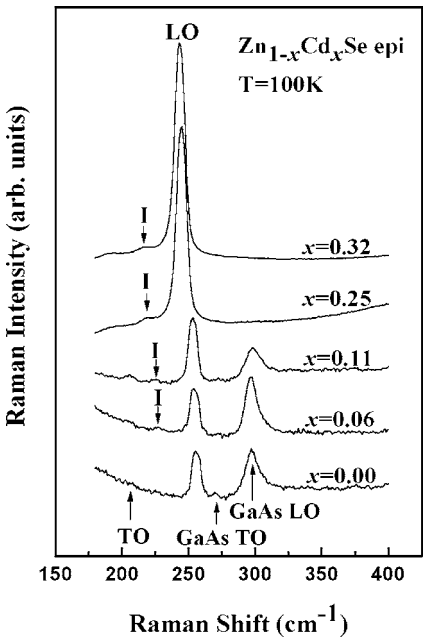

FIG. 3. Raman spectra of $Zn_{1-x}Cd_xSe$ epilayers ($0 \leqq x \leqq 0.32$) at 100 K and ambient pressure. The impurity (*I*) modes, indicated by black arrows, appear at low temperature. The LO and TO phonons of the GaAs substrate are also labeled.

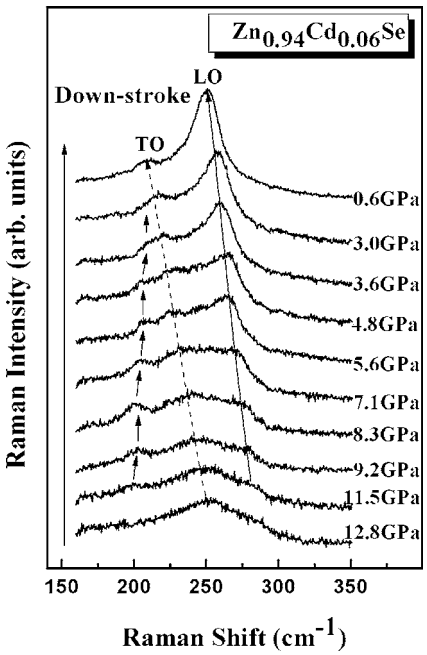

FIG. 5. Down-stroke pressure-dependent Raman spectra of $Zn_{1-x}Cd_xSe$ ($x=0.06$) at room temperature. The splitting of the TO phonon, labeled by black arrows, was observed clearly as the pressure was released.

skin depth (or penetration depth) of the metal into which the laser penetrates is merely several tens of angstroms.[10,11] Similar experimental results were obtained from our samples with low Cd content ($x \leqq 0.18$) and in earlier investigations of nonmagnetic and magnetic II–VI ternary compounds, ZnFeSe,[10] ZnSeTe,[11] and ZnMnSe[12] crystals.

In our previous investigations, the TO phonon splitting occurred in the up-stroke pressure process and was attributed to the pressure-induced formation of an additional phase. Despite numerous careful searches; however, no TO splitting was observed in any of the studied $Zn_{1-x}Cd_xSe$ samples during the up-stroke process, which were examined several times by reloading them and changing the pressure medium to de-ionized (DI) water. Nevertheless, in the down-stroke process of $Zn_{0.94}Cd_{0.06}Se$, shown in Fig. 5, a split TO phonon mode begins to develop as the pressure is reduced to around 11.5 GPa. It becomes more pronounced at 8.3 GPa. The split TO phonon mode is slightly blueshifted and its intensity falls as the pressure is released. The splitting of the TO mode in the down-stroke process also implies the formation of an additional high-pressure phase. Recent EDXD experiments by Pellicer-Porres *et al.*[20,21] demonstrated that ZnSe and $ZnSe_xTe_{1-x}$ exhibited a cinnabar structure between the ZB and RS structures, becoming apparent only in the down-stroke process. Côté *et al.*[22] also theoretically calculated the existence of a fourfold-coordinated cinnabar phase between ZB and RS phases, which could be found in the down-stroke process. Accordingly, this work presents the observation of a cinnabar phase in $Zn_{1-x}Cd_xSe$ by Raman scattering in the down-stroke process.

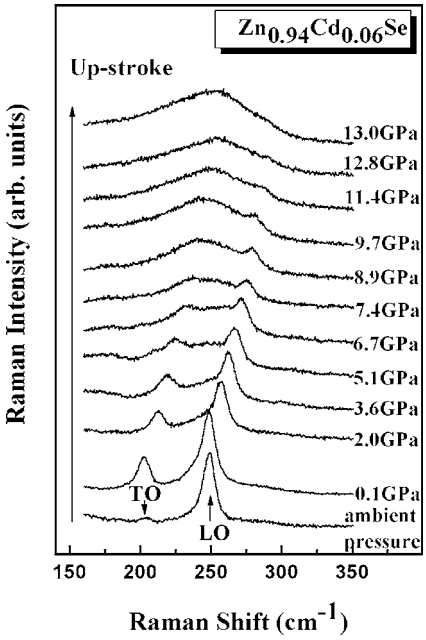

FIG. 4. Up-stroke pressure-dependent Raman spectra of $Zn_{1-x}Cd_xSe$ ($x=0.06$) at room temperature. The LO phonon disappears at around 13.0 GPa, revealing a structural change from semiconductor to metal.

Table II lists the pressure-dependent LO phonon frequencies obtained by fitting a quadratic polynomial equation to our measurements,

$$\omega_{LO} = \omega_0 + ap + bp^2, \tag{1}$$

where ω_0 is the LO phonon frequency at ambient pressure, p is the pressure in gigapascal, and a and b are the vibrational pressure coefficients for this mode. The pressure dependence of a mode frequency ω_{LO} can be defined in terms of the dimensionless Grüneisen parameter (γ_{LO}), which is given by[23]

TABLE II. Pressure-dependent LO phonon frequencies (ω_{LO}) $d\omega_{LO}/dp$, calculated mode Grüneisen parameters (γ_{LO}), and phase transition pressures for $Zn_{1-x}Cd_xSe$ epilayers.

Cd content (x)	ω_{LO} (cm^{-1})	$d\omega_{LO}/dp$ (cm^{-1}/GPa)	Grüneisen parameter γ_{LO}	Phase transition pressure (GPa)
0	$252.2+3.31p-0.04p^2$	$3.31-0.08p$	0.82	13.6±0.2
0.06	$248.4+3.99p-0.06p^2$	$3.99-0.12p$	1.00	12.9±0.1
0.11	$247.9+4.26p-0.09p^2$	$4.26-0.18p$	1.07	12.6±0.1
0.18	$244.6+4.51p-0.06p^2$	$4.51-0.12p$	1.15	12.0±0.2
0.25	$242.1+3.82p-0.09p^2$	$3.82-0.18p$	0.98	10.6±0.4
0.32	$239.1+4.53p-0.09p^2$	$4.53-0.18p$	1.18	9.4±0.2

$$\gamma_{LO} = -\left(\frac{d \ln \omega_{LO}}{d \ln V}\right) = \frac{1}{\beta}\frac{\partial \ln \omega_{LO}}{\partial p} = \left(\frac{K_0}{\omega_{LO}}\right)\left(\frac{d\omega_{LO}}{dp}\right), \quad (2)$$

where K_0 is the bulk modulus, defined as the inverse of the isothermal volume compressibility (β), and V is the molar volume in cm^3/mol. Since the bulk modulus (K_0) of $Zn_{1-x}Cd_xSe$ is unknown, $K_{0(ZnSe)}=62.4$ GPa is used.[24] Table II presents the γ_{LO} values of all samples at ambient pressure. $d\omega/dp=3.31$ cm^{-1}/GPa and $\gamma_{LO}=0.82$ and $d\omega/dp=4.53$ cm^{-1}/GPa and $\gamma_{LO}=1.18$ are obtained for ZnSe and $Zn_{1-x}Cd_xSe$ ($x=0.32$), respectively. Camacho *et al.*[18] noted that no pressure-dependent Raman results for bulk CdSe or epilayer had been published. However, Alivisatos *et al.*[25] found $d\omega/dp=4.30$ cm^{-1}/GPa and $\gamma_{LO}=1.1$ for ZB-phase CdSe nanocrystals. The ionization of the lattice can be deduced from γ_{LO},[26] and the ionicity (f_i) of CdSe (0.70) is larger than that of ZnSe (0.63).[27] By contrast, the higher Cd concentration samples exhibit larger lattice ionization and higher pressure variation on the phonon frequency. In Table II, we can see that the applied pressure tends to reduce the variation of phonon frequency and the lattice ionization due to the second negative term of $d\omega/dp$.

Figure 6 shows the pressure-dependent Raman spectra of $Zn_{1-x}Cd_xSe$ epilayer ($x=0.25$) at room temperature. The TO phonon is not found and the intensity of LO phonons does not monotonously decline as the pressure increases. Samples with a high Cd content ($x=0.18$, and 0.32) exhibit a similar trend, because of the pressure-driven RRS effect, which occurs when the incident laser energy is sufficiently close to the energy of the electronic excitations, described as

$$h\nu_{laser} - mh\nu_{LO} \approx E_g - E_{exc}, \quad (3)$$

where $h\nu_{laser}$ is the photon energy of the incident laser (2.41 eV), $E_g - E_{exc}$ is the electronic transition energy of exciton peak, $h\nu_{LO}$ is the energy of the LO phonon, and m denotes the overtone order of LO phonons. The exciton energy of $Zn_{1-x}Cd_xSe$ was controlled by tuning the Cd concentration during the growth, or by manipulating the pressure and temperature of the sample chamber. In this investigation, $h\nu_{laser}$ was fixed at 2.41 eV and the exciton energy increased with pressure. As the external pressure was gradually tuned toward 6.6 GPa, the exciton energy approached the laser energy and an increase in intensity of LO phonon was observed. By further increasing the pressure, the exciton energy exceeds the incident laser energy (at around 7.5 GPa in Fig. 6) and begins to move away from the RRS condition, and the intensity of LO phonon decreases monotonously as the pressure increases. At around 11.0 GPa, the LO phonon disappears, revealing the structure transformation from the semiconductor to the metal phase.

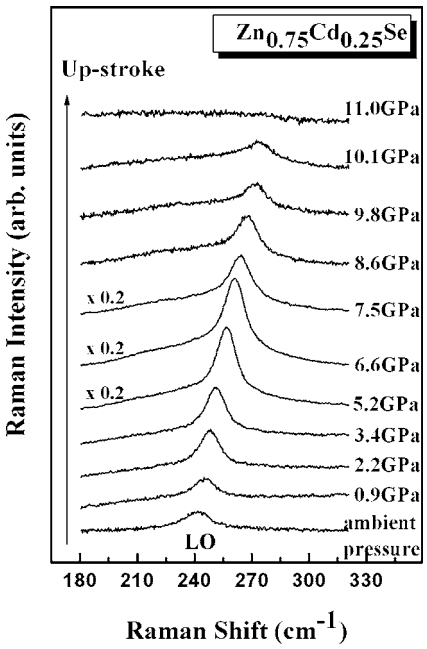

FIG. 6. Up-stroke pressure-dependent Raman spectra of $Zn_{1-x}Cd_xSe$ ($x=0.25$) at room temperature. The pressure-driven resonant Raman scattering effect occurred as the pressure was increased. The LO phonon was found to disappear at about 11.0 GPa.

Figure 7 displays the pressure-dependent PL spectra of the $Zn_{1-x}Cd_xSe$ epilayer ($x=0.25$) at 300 K. At 0.2 GPa, the broad peak at 2.08 eV is attributed to the near band edge (NBE) emission. As the pressure is increased to 2.2 GPa, the NBE emission shifts to higher energy. Further increasing the pressure causes the NBE emission to overlap the LO phonon peaks. The intensity of the LO phonon peaks of the Stokes side increases and the RRS effect occurs. The inset in Fig. 7 plots the peak energies of the room-temperature PL spectra before the phase transition as a function of pressure. The PL spectra were excited using an Ar^+ 488 nm laser line (2.54 eV) to observe the NBE emission above the 2.41 eV energy of the Ar^+ 514.5 nm laser line, which was used to excite phonon Raman scattering. As the pressure further increases to above 6.6 GPa, far from the RRS condition, the intensity of the 1LO phonon decreases abruptly and the PL spectra disappears because the NBE energy exceeds the excitation laser energy. When the pressure reaches the critical value for the phase transition (11.0 GPa), the LO phonons at both sides of Raman spectra disappears. This result is a strong evidence of the semiconductor-to-metal phase transition. The phase transition pressure of this sample, at which the LO phonon disappeared, was also verified using a 632.8 nm ruby laser as an excitation source, this wavelength is far from what is associated with the RRS effect.

The critical pressures of semiconductor-to-metal phase transition of all $Zn_{1-x}Cd_xSe$ epilayers discussed herein are

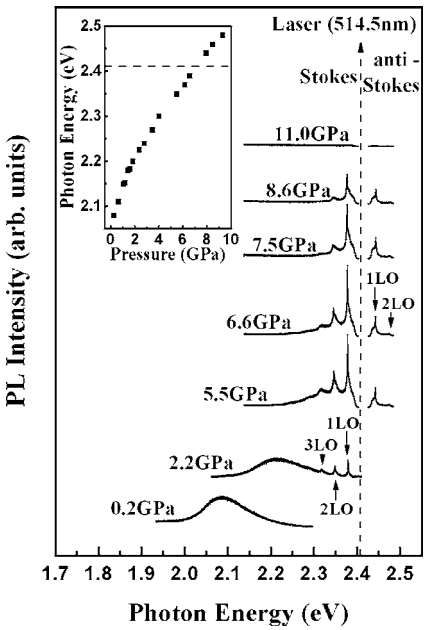

FIG. 7. Pressure-dependent photoluminescence spectra of $Zn_{1-x}Cd_xSe$ ($x=0.25$) at 300 K. The 514.5 nm (2.41 eV) Ar^+ laser was fixed as an excitation source. The black dashed arrow at 2.41 eV labels the energy of the excitation laser, whereas the Stokes and anti-Stokes Raman spectra occur at the lower and higher energy sides of the laser, respectively. The inset plots the pressure dependence of PL energies, and the dashed line indicates the energy of the excitation laser.

listed in Table II. As the Cd concentration increases to 0.32, the phase transition pressure falls from 13.6 to 9.4 GPa. Figure 8 plots the decline in the phase transition pressure as a function of x. The solid line represents a quadratic fit, given by $Pt(GPa)=13.6-6.8x-20.3x^2$. The fall of Pt with x suggests a reduction in structural stability. The structure becomes destabilized as the substituted element content increases, this relationship has been observed in other ZnSe-based ternary semiconductors. For instance, Yang *et al.*

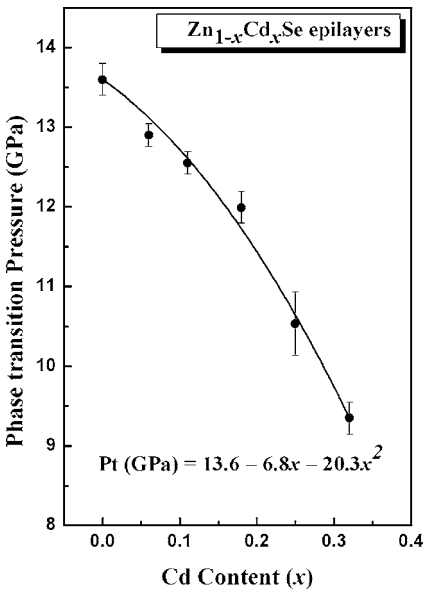

FIG. 8. Cd concentration (x)-dependent phase transition (semiconductor-to-metal) pressure of $Zn_{1-x}Cd_xSe$ epilayers. The solid curve represents a quadratic polynomial fit.

found that for $ZnSe_{1-x}Te_x$ epilayers with x up to 0.54, the critical pressure of semiconductor-to-metal phase transition decreased from 13.7 to 7.3 GPa. For $Zn_{1-x}Mn_xSe$ crystals, the structural transition from zinc blende (B_3) to rocksalt (B_1) occurred at about 11.8 and 9.9 GPa for $x=0.07$ and 0.24, respectively.[11,12]

IV. CONCLUSIONS

The pressure-dependent Raman and PL spectra of $Zn_{1-x}Cd_xSe$ epilayers ($0 \leqq x \leqq 0.32$) were investigated. Low-temperature experiments reveal that the optical phonons of $Zn_{1-x}Cd_xSe$ exhibit intrinsic intermediate-mode behavior. The splitting of the TO mode in the down-stroke pressurized process may have been caused by the formation of an additional high-pressure phase. The pressure-dependent LO phonon frequencies are fitted with a quadratic polynomial equation and the Grüneisen parameters are obtained. The pressure-driven RRS effect was observed in samples with a high Cd concentration ($x \geqq 0.18$). Both the Stokes and anti-Stokes sides of the LO phonons disappear as the crystal structure changes from semiconductor-to-metal phase. The critical pressure of semiconductor-to-metal phase transition is found to decrease as the Cd content increases.

ACKNOWLEDGMENTS

This work was supported by MOE-ATU and the National Science Council under Grant No. NSC 95-2112-M-009-047.

[1] M. A. Haase, J. Qiu, J. M. Depuydt, and H. Cheng, Appl. Phys. Lett. **59**, 1272 (1991).
[2] J. Ding, H. Jeon, T. Ishihara, M. Hagerott, A. V. Nurmikko, H. Luo, N. Samarth, and J. K. Furdyna, Phys. Rev. Lett. **69**, 1707 (1992).
[3] W. Faschinger and J. Nürnberger, Appl. Phys. Lett. **77**, 187 (2000).
[4] S.-B. Che, I. Nomura, A. Kikuchi, and K. Kishino, Appl. Phys. Lett. **81**, 972 (2002).
[5] J. Avendaño-López, F. L. Castillo-Alvarado, A. Escamilla-Esquivel, G. Contreras-Puente, J. Ortiz-López, and O. Zelaya-Angel, Solid State Commun. **100**, 33 (1996).
[6] U. Lunz, J. Kuhn, F. Goschenhofer, U. Schüssler, S. Einfeldt, C. R. Becker, and G. Landwehr, J. Appl. Phys. **80**, 6861 (1996).
[7] N. Samarth, H. Luo, J. K. Furdyna, R. G. Alonso, Y. R. Lee, A. K. Ramdas, S. B. Qadri, and N. Otsuka, Appl. Phys. Lett. **56**, 1163 (1990).
[8] S. Fujita, Y. Wu, Y. Kawakami, and S. Fujita, J. Appl. Phys. **72**, 5233 (1992).
[9] S. B. Qadri, E. F. Skelton, A. W. Webb, N. Moulton, J. Z. Hu, and J. K. Furdyna, Phys. Rev. B **45**, 5670 (1992).
[10] C.-M. Lin, D.-S. Chuu, T.-J. Yang, W.-C. Chou, J. Xu, and E. Huang, Phys. Rev. B **55**, 13641 (1997).
[11] C. S. Yang, W. C. Chou, D. M. Chen, C. S. Ro, J. L. Shen, and T. R. Yang, Phys. Rev. B **59**, 8128 (1999).
[12] C. S. Yang, C. S. Ro, W. C. Chou, C. M. Lin, D. S. Chuu, J. Hu, E. Huang, and J. Xu, J. Appl. Phys. **85**, 8092 (1999).
[13] A. K. Arora and T. Sakuntala, Phys. Rev. B **52**, 11052 (1995).
[14] G. J. Piermarini, S. Block, J. D. Barnett, and R. A. Forman, J. Appl. Phys. **46**, 2774 (1975).
[15] H. K. Mao, P. M. Bell, J. W. Shaner, and D. J. Steinberg, J. Appl. Phys. **49**, 3276 (1978).
[16] W. Meredith, G. Horsburgh, G. D. Brownlie, K. A. Prior, B. C. Cavenett, W. Rothwell, and A. J. Dann, J. Cryst. Growth **159**, 103 (1996).
[17] R. G. Alonso, E.-K. Suh, A. K. Ramdas, N. Samarth, H. Luo, and J. K. Furdyna, Phys. Rev. B **40**, 3720 (1989).
[18] J. Camacho, I. Loa, A. Cantarero, K. Syassen, I. Hernández-Calderón, and

L. González, Phys. Status Solidi B **235**, 432 (2003).
[19]W. S. Li, Z. X. Shen, D. Z. Shen, and X. W. Fan, J. Appl. Phys. **84**, 5198 (1998).
[20]J. Pellicer-Porres, A. Segura, V. Muñoz, J. Zúñiga, J. P. Itié, A. Polian, and P. Munsch, Phys. Rev. B **65**, 012109 (2001).
[21]J. Pellicer-Porres, D. Martínez-García, Ch. Ferrer-Roca, A. Segura, V. Muñoz-Sanjosé, J. P. Itié, A. Polian, and P. Munsch, Phys. Rev. B **71**, 035210 (2005).
[22]M. Côté, O. Zakharov, A. Rubio, and M. L. Cohen, Phys. Rev. B **55**, 13025 (1997).
[23]M. Blackman and W. B. Daniels, in *Light Scattering in Solids IV*, edited by M. Cardona and G. Güntherodt (Springer, Berlin, 1984), Chap. 8.
[24]S. Ves, K. Strössner, N. E. Christensen, C. K. Kim, and M. Cardona, Solid State Commun. **56**, 479 (1985).
[25]A. P. Alivisatos, T. D. Harris, L. E. Brus, and A. Jayaraman, J. Chem. Phys. **89**, 5979 (1988).
[26]R. W. Meulenberg and G. F. Strouse, Phys. Rev. B **66**, 035317 (2002).
[27]J. C. Phillips, Phys. Rev. Lett. **27**, 1197 (1971).